

## Hydrothermal Synthesis of TiO<sub>2</sub> Nanorod Bundles in the Presence of Tetramethylammonium Hydroxide

Teming Lai,<sup>\*1,2</sup> Long Yi,<sup>1,2</sup> and Wenxia Yang<sup>1,2</sup>

<sup>1</sup>College of Chemistry and Life Science, Gannan Normal University, Ganzhou 341000, P. R. China

<sup>2</sup>Research Center of Navel Orange Engineering and Technology JiangXi, Gannan Normal University, Ganzhou 341000, P. R. China

(Received November 19, 2009; CL-091025; E-mail: laitm82@sina.com)

Highly crystallized anatase TiO<sub>2</sub> nanorod bundles have been prepared by a hydrothermal method in the presence of tetramethylammonium hydroxide (TMAOH) for the first time. TMAOH plays a structural template role to modify the TiO<sub>2</sub> particle shape to nanorod. Many nanorods stick together in the middle, obtaining a special nanorod bundle. The TiO<sub>2</sub> nanorod bundles show relatively higher photocatalytic activity than Degussa P25 evaluated via the degradation of phenol.

Over the past decade, there has been growing interest in controlling the size and shape of nanomaterials, because these parameters play a key role in their physical and chemical properties.<sup>1,2</sup> Particularly, the synthesis of one-dimensional (1-D) semiconducting nanostructures such as nanorods and nanowires has received much attention due to their peculiar electrical transportation properties, field emission properties and potential applications in nanodevices.<sup>3,4</sup> So far, many methods have been used to prepare 1-D nanostructure semiconductors, such as electrodeposition,<sup>5</sup> template-directed synthesis,<sup>6,7</sup> laser-assisted catalytic growth,<sup>8</sup> solution-phase methods,<sup>9</sup> and the chemical vapor deposition (CVD) route.<sup>2</sup> The solution-phase method, avoiding complicated processes and special instruments, is favorable for producing 1-D nanostructure materials in terms of its low cost and convenience.<sup>10</sup>

Recently, 1-D structures of nanosize TiO<sub>2</sub> have attracted great research interests because of their size- and dimensionality-dependent physicochemical properties and extensive potential applications in the field of solar-energy conversion, lithium batteries, and supercapacitors.<sup>11,12</sup> TMAOH is a strong organic alkali which used in TiO<sub>2</sub> syntheses.<sup>13–15</sup> For example, Moritz and his partners<sup>13</sup> synthesized anatase superlattices with packed hexagonal nanocrystallites. Burnside et al.<sup>14</sup> obtained a TiO<sub>2</sub> nanorod array in thin films by the same method. Chen et al.<sup>15</sup> synthesized well-aligned nanosquares and nanorods. Differently, in our work, nanorod bundle-shaped anatase was fabricated in the presence of TMAOH for the first time.

All reagents were of analytical purity, purchased from Shanghai Chemical Reagent Co., Ltd. of China and used without further purification. In a typical synthesis, 3.4 mL of tetrabutyl titanate (Ti(OBu)<sub>4</sub>) was rapidly added to 100 mL of distilled water and stirred for 2 h. A white precipitate formed immediately upon addition of the Ti(OBu)<sub>4</sub>. The resulting white products were filtered and washed until the electric conductivity of the filtrate was below 100 μs cm<sup>-1</sup>. Under continuous magnetic stirring, the filtered wet gel was added to 30 mL of 1.732 g TMAOH solution. Then the formed peptization was heated at 90 °C for 6 h. The resultant product was transferred into a 50-mL Teflon-lined stainless autoclave 70% filled. The final product was thus obtained after heating at 160 °C for 4 h.

The XRD analysis was performed using a Rigaku D/MAX-2000 X-ray diffractometer at room temperature, operating at 30 kV and 30 mA, using Cu Kα radiation ( $\lambda = 0.15418$  nm). The TEM image was recorded on a JEOL JEM-200 CX microscope at an acceleration voltage of 200 kV. FT-IR spectra were measured on an AVATAR 370-IR spectrometer (Thermo Nicolet, America) with a wavenumber range of 4000 to 400 cm<sup>-1</sup>. Phenol is a representative phenolic compound in aqueous solution and a major industrial pollutant. Hence, the photocatalytic activity of the TiO<sub>2</sub> photocatalysts was evaluated by photocatalytic degradation of phenol. The initial concentration of phenol was 10 mg L<sup>-1</sup>, equivalent to 1.0 g L<sup>-1</sup> of TiO<sub>2</sub> in aqueous solution. A 16 W UV lamp (365 nm) was used. The samples were immediately centrifuged and the phenol concentration of the solution was detected by a UV-2501 PC spectrometer (Shimadzu, Japan) at a wavelength of 200–400 nm.

Figure 1 shows the XRD pattern of the obtained sample. All diffraction peaks correspond to anatase phase without any other impurity phase. The diffraction lines are relatively broad, indicating the nanosize of high crystallinity. The particle size of anatase calculated using the Scherer formula<sup>16</sup> is 23.0 nm.

Further structural characterization of the TiO<sub>2</sub> sample was carried out using TEM image analysis. Figure 2 shows the TEM image of the product. As shown in the TEM image, many nanorods stick together in the middle and display uniform broom-like bundles with two ends fanning out. The nanorod bundle has a width of 5–20 nm and length of 270–430 nm. The presence of TMAOH, as a structural template, provide organic cation to assist and direct the polycondensation process,<sup>15</sup> resulting in the formation of nanorod bundle anatase. This may contribute to the longer heat time at 90 °C before hydrothermal process. A detailed investigation for the effect of TMAOH in determining bundle-shaped TiO<sub>2</sub> is now in progress.

The FT-IR spectroscopy is shown in Figure 3. The bands observed at 3405 and 1630 cm<sup>-1</sup> are due to stretching and

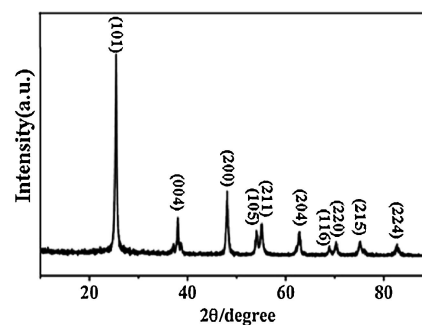
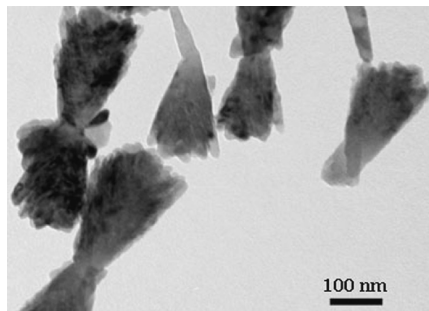
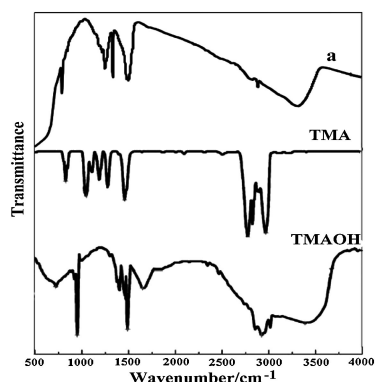


Figure 1. XRD pattern of the TiO<sub>2</sub> nanorod bundles.



**Figure 2.** TEM image of the TiO<sub>2</sub> nanorod bundles.



**Figure 3.** FT-IR spectrum of the TiO<sub>2</sub> nanorod bundles (a) and the standard spectra of TMAOH and TMA.

bending vibration modes of H<sub>2</sub>O molecules while the band at 2925 and 2850 cm<sup>-1</sup> belong to antisymmetric and symmetric C–H stretching vibrations of the TMAOH and the band at 2960 cm<sup>-1</sup> is attributed to –CH<sub>3</sub> groups.<sup>17</sup> Comparing with the standard spectra of TMAOH and TMA, the spectrum of TiO<sub>2</sub> nanorod bundles in the range of 1000–2000 cm<sup>-1</sup> is closer to that of TMA. The bands below 1000 cm<sup>-1</sup> are ascribed to the vibrations of Ti–O–Ti network in anatase.

The photocatalytic activity of the two TiO<sub>2</sub> photocatalysts is shown in Figure 4. The blank test in the absence of TiO<sub>2</sub> photocatalyst was carried out. After photolytic reaction for 6 h, the concentration of phenol solution was almost unchanged. In the presence of TiO<sub>2</sub> nanorod bundles, the photocatalytic degradation of phenol is 62.3% while the photocatalytic efficiency of P25 is 58.6%. Many factors can affect the photocatalytic activity. Many studies<sup>18,19</sup> reported that the bicrystalline framework, high crystallinity, large surface area, mesoporous structure, high visible light absorption, and the nanocrystals with abundant surface states can make the TiO<sub>2</sub> nanocrystals possess enhanced photocatalytic activities. Therefore, the relatively high photocatalytic activity may be due to the higher surface-to-volume ratio, large surface area, and the mesoporous structure, which would guarantee a high density of active sites available for surface reactions as well as a high interfacial charge-carrier transfer rate. The increased delocalization of carriers in rods would reduce the e<sup>-</sup>/h<sup>+</sup> recombination to ensure a more efficient charge separation.<sup>17,20</sup> It is expected that large surface area contributes to high photocatalytic activity of TiO<sub>2</sub> nanocrystals with certain crystallinity by creating more possible reactive sites on the surface of photocatalyst. Kominami

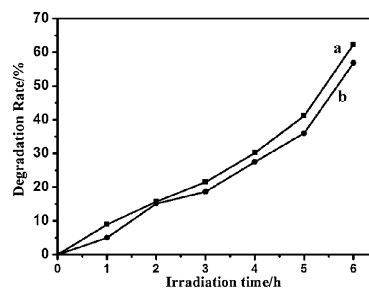


**Figure 4.** Process of photocatalytic degradation of phenol under UV light illumination of TiO<sub>2</sub> nanorod bundles (a) and Degussa P25 (b).

et al.<sup>21,22</sup> also reported that the higher activity of the TiO<sub>2</sub> photocatalyst is attributed to both high crystallinity and large surface area. From the experimental result we obtained, the photocatalyst of TiO<sub>2</sub> nanorod bundles possess relatively higher surface area of 105.6 m<sup>2</sup> g<sup>-1</sup> while the value of P25 is 51 m<sup>2</sup> g<sup>-1</sup>. Moreover, the nanorod bundles may stagger to form porous structure, which could adsorb more pollutants to increase the photocatalytic activity.

In summary, TiO<sub>2</sub> nanorod bundles have been successfully fabricated by a simple hydrothermal process in the presence of TMAOH. The presence of TMAOH accelerates the formation of crystalline anatase and modifies the shape of particles as a structural template. The nanorod bundle-shaped TiO<sub>2</sub> exhibits relatively higher photocatalytic activity than Degussa P25 evaluated via the degradation of phenol.

#### References and Notes

- X. Duan, Y. Huang, R. Agarwal, C. M. Lieber, *Nature* **2003**, *421*, 241.
- M. H. Huang, S. Mao, H. N. Feick, H. Q. Yan, Y. Y. Wu, H. Kind, E. Weber, R. Russo, P. Yang, *Science* **2001**, *292*, 1897.
- H. Zhang, D. Yang, Y. Ji, X. Ma, J. Xu, D. Que, *J. Phys. Chem. B* **2004**, *108*, 1179.
- H. Zhang, D. Yang, Y. Ji, X. Ma, J. Xu, D. Que, *J. Phys. Chem. B* **2004**, *108*, 3955.
- D. Xu, Y. Xu, D. Chen, G. Guo, L. Gui, Y. Tang, *Adv. Mater.* **2000**, *12*, 520.
- K. M. Ryan, D. Ertz, H. Olin, M. A. Morris, J. D. Holmes, *J. Am. Chem. Soc.* **2003**, *125*, 6284.
- C. Tang, S. Fan, M. Lamy de la Chapelle, H. Dang, P. Li, *Adv. Mater.* **2000**, *12*, 1346.
- A. M. Morales, C. M. Lieber, *Science* **1998**, *279*, 208.
- B. Gates, Y. D. Yin, Y. N. Xia, *J. Am. Chem. Soc.* **2000**, *122*, 12582.
- Z. H. Wang, X. Y. Chen, J. W. Liu, X. G. Yang, Y. T. Qian, *Inorg. Chem. Commun.* **2003**, *6*, 1329.
- M. Adachi, Y. Murata, J. Takao, J. Jiu, M. Sakamoto, F. Wang, *J. Am. Chem. Soc.* **2004**, *126*, 14943.
- J. Joo, S. G. Kwon, T. Yu, M. Cho, J. Lee, J. Yoon, T. Hyeon, *J. Phys. Chem. B* **2005**, *109*, 15297.
- T. Moritz, J. Reiss, K. Diesner, D. Su, A. Chemseddine, *J. Phys. Chem. B* **1997**, *101*, 8052.
- S. D. Burnside, V. Shklover, C. Barbé, P. Comte, F. Arendse, K. Brooks, M. Grätzel, *Chem. Mater.* **1998**, *10*, 2419.
- Y. X. Chen, X. He, X. J. Zhao, Q. H. Yuan, X. Y. Gu, *J. Colloid Interface Sci.* **2007**, *310*, 171.
- TiO<sub>2</sub> (anatase), JCPDF card No. 21-1272.
- P. D. Cozzoli, A. Kornowski, H. Weller, *J. Am. Chem. Soc.* **2003**, *125*, 14539.
- G. Liu, Z. G. Chen, C. L. Dong, Y. N. Zhao, F. Li, G. Q. Lu, H.-M. Cheng, *J. Phys. Chem. B* **2006**, *110*, 20823.
- G. Liu, X. W. Wang, L. Z. Wang, Z. G. Chen, F. Li, G. Q. Lu (Max), H.-M. Cheng, *J. Colloid Interface Sci.* **2009**, *334*, 171.
- L. Manna, E. C. Scher, A. P. Alivisatos, *J. Am. Chem. Soc.* **2000**, *122*, 12700.
- H. Kominami, J. Kato, Y. Takada, Y. Doushi, B. Ohtani, S. Nishimoto, M. Inoue, T. Inui, Y. Kera, *Catal. Lett.* **1997**, *46*, 235.
- H. Kominami, H. Kumamoto, Y. Kera, B. Ohtani, *J. Photochem. Photobiol., A* **2003**, *160*, 99.